Potential crosstalk of Ca^{2+}-ROS-dependent mechanism involved in apoptosis of Kasumi-1 cells mediated by heme oxygenase-1 small interfering RNA

SIXI WEI[1,3-5], YATING WANG[1,4,5], QIXIANG CHAI[1,4,5], QIN FANG[2], YAMING ZHANG[1,4,5] and JISHI WANG[1,4,5]

Departments of [1]Hematology, [2]Pharmacy and [3]Clinical Biochemistry, Affiliated Hospital of Guiyang Medical College; [4]Hematopoietic Stem Cell Transplantation Center of Guizhou Province; [5]Key Laboratory of Hematological Disease Diagnostic and Treat Centre of Guizhou Province, Guiyang 550004, P.R. China

Abstract. Acute myeloid leukemia (AML) requires new therapies on the molecular level. Downregulation of heme oxygenase-1 (HO-1) by gene silencing improves the sensitivity of tumor cells to chemotherapy drugs and promotes apoptosis. For the first time, we verified that endoplasmic reticulum and mitochondrial apoptotic pathways were activated by small interfering RNA that targeted-silenced the expression of HO-1 in AML-M2 Kasumi-1 cells. Ca^{2+} was prone to accumulation and reactive oxygen species were easily generated, while mitochondrial transmembrane potential was reduced. Thus, cytochrome c was released from mitochondria to the cytoplasm and caspases were activated for the following cascade to facilitate apoptosis.

Introduction

Acute myeloid leukemia (AML) is a group of hematopoietic malignancies arising from the abnormalities of proliferation, differentiation, or survival of myeloid progenitors. Clinically, the complete remission rate is high among AML patients using the current chemotherapy, and a recent study in China showed that the 3-year disease-free survival rate was only 11% (1). Moreover, as one of the treatments for AML, hematopoietic stem cell transplantation requires strict selection of donors and recipients. Acute and chronic graft versus host diseases also affect the survival rate and survival quality of patients (2).

Correspondence to: Professor Jishi Wang, Department of Hematology, Affiliated Hospital of Guiyang Medical College, Guiyang 550004, P.R. China
E-mail: wangjishi9646@163.com
E-mail: wangjishidh@126.com

Therefore, potential therapeutic targets for AML are the hot topics of current research.

Heme oxygenase-1 (HO-1), the rate-limiting enzyme in protoheme catabolism, is one of the most important regulatory enzymes for oxidation. Its expression can be induced by a variety of external factors (heavy metals, protoheme, hypoxia, NO, prostaglandins, cytokines and antioxidant). HO-1 is mainly involved in iron recycle and maintenance of normal intracellular homeostasis under normal physiological conditions (3). Under pathological or stress conditions, HO-1 mainly protects cells, resists apoptosis, promotes cell proliferation and mitigates inflammation (4). In recent years, the relationships between high expression of HO-1 and drug resistance and promotion of cell proliferation have been extensively studied (5-8). Besides, HO-1 is associated with the occurrence and development of hematological tumors. When highly expressed, it protects leukemia cells from chemotherapy drugs, reduces apoptosis and enhances drug resistance (9-11). Therefore, the role of HO-1 in leukemia research and whether HO-1 can be used as a potential target for leukemia treatment are worthy of in-depth studies. Our previous studies have shown that HO-1 was highly expressed in *de novo* AML and chronic myeloid leukemia (CML), confirming that HO-1 was involved in regulating the survival and apoptosis of CML cells and was associated with CML disease progression and drug resistance (12-14). Since AML-related studies remain rare and the mechanism for its effects on cell survival has not yet been elucidated, it is of great significance to discuss the influence of HO-1 on the biological effects of AML and possible mechanisms, so as to provide experimental basis for the targeted treatment of AML.

Based on our previous findings, Kasumi-1 cells (AML-M2 cell line) infected with lentiviral vector carrying HO-1 small interfering RNA (siRNA) were selected in this study to explore the influences of targeted-silenced HO-1 on the survival and apoptosis of Kasumi-1 cells and the most likely mechanism. We tried to clarify the possible pathway involved in Kasumi-1 cell apoptosis mediated by HO-1 siRNA, with daunorubicin (DNR) treatment before and after silencing of HO-1 expression.

Materials and methods

Cell culture. The human AML-M2 cell line, Kasumi-1 cells (15) were cryopreserved in the center laboratory of Hematopoietic Stem Cell Transplantation Center of Guizhou Province (Guiyang, China). Cells were maintained in Roswell Park Memorial Institute-1640 (RPMI-1640) medium containing 10% fetal bovine serum, 100 U/ml penicillin and 100 g/ml streptomycin at 37˚C in an incubator containing 5% CO_2 and humidified air. The medium and antibiotics were from Sijiqing (Hangzhou Tianhang Biological Technology Co., Ltd., Zhejiang, China). The study was approved by the ethics committee of Hospital affiliated to Guiyang Medical College (Guiyang, China).

Chemicals and antibodies. Daunorubicin (DNR), N-acetyl-L-cysteine (NAC) and BAPTA-AM were respectively purchased from Sigma (St. Louis, MI, USA), Beyotime Institute of Biotechnology (Haimen, Jiangsu, China) and Dojindo Molecular Technologies (Kumamoto, Japan). Cytoplasmic and mitochondrial protein extraction kit was purchased from Sangon Biotech Co., Ltd. (Shanghai, China). Antibodies for western blot analysis were obtained from Cell Signaling Technology (Beverly, MA, USA) and secondary antibodies were purchased from Santa Cruz Biotechnology (Santa Cruz, CA, USA).

Reagents preparation and processing. According to the instructions, DNR was dissolved with ddH_2O to prepare a 1 g/ml stock solution. Based on the preliminary results, the stock solution was further diluted into working solutions at the final concentrations of 5, 7.5, 10 and 12.5 μg/ml by RPMI-1640 medium. NAC was dissolved with RPMI-1640 to prepare a 1 mol/l stock solution that was diluted into working solutions at the final concentration of 10 mmo/l. BAPTA-AM was dissolved with dimethyl sulfoxide (DMSO) (Solarbio Science & Technology Co., Ltd., Beijing, China) to form a 1 mol/l stock solution, which was then diluted into working solutions with Hank's balanced salt solution (HBSS) (Life Technologies, Foster City, CA, USA) at the final concentration of 10 μmol/l. Corresponding blank controls were set for different treatments.

Cell transfection. HO-1 (NM_002133.2)-targeted siRNA, pRNAi-siHO-1-GFP and pRNAi-GFP (lentiviral vector carrying with/without HO-1 siRNA), were designed and purchased from Biomics Biotechnologies (Nantong) Co., Ltd. (Jiangsu, China). According to the results of preliminary experiments, the most effective one (5'-AAGCUUUCUGGU GGCGACAGU-3') was chosen in our study. Kasumi-1 cells in the log phase were planted at the concentration of $1x10^6$/well in 6-well plate after overnight culture and were then transfected with pRNAi-GFP (with/without siHO-1) at multiplicities of infection of 8 in serum-free medium. Polybrene (5 μg/ml) (Sigma) was added to improve transfection efficiency as enhancing reagent. After 10 h, the medium was changed for complete medium, and the cells without intervention were used as blank control group. After transfection for 24, 48 and 72 h, infection efficiency of lentivirus was observed by fluorescence microscopy (Olympus, Tokyo, Japan) and flow cytometry (FCM) with FL-1 channel.

Survival analysis with MTT assay. Kasumi-1 cells in the log phase were inoculated into 96-well plates with the density of $1x10^4$/well, and treated with different interventions. Serum-free RPMI-1640 was added for the blank control group until the total volume of 200 μl in each well. Six replicates were set and the cells were cultured for 24, 48 and 72 h. At the end of culture, the medium in each well was replaced with 200 μl of fresh medium containing MTT (Solarbio). After incubation at 37˚C for 4 h, cells were centrifuged (1,000 r/min, 10 min) and the supernatant was discarded. The reaction was terminated by adding 200 μl/well of DMSO, and the resultant solution was subjected to vibrate-shaking for 10 min to fully dissolve the crystals. The absorbance at 570 nm (A_{570}) of each sample well was measured using an automated 96-well plate reader. All assays were performed in triplicate. The inhibition rate was calculated using the following equation:

$$\text{Inhibition rate (\%)} = 1 - A_{treated}/A_{control} \times 100\%$$

Real-time PCR detection. Total RNA was extracted using TRIzol® Reagent (Invitrogen Life Technologies, Carlsbad, CA, USA). RNA was reverse transcribed into cDNA using a reverse transcription kit (Promega Corp., Madison, WI, USA), which was stored at -20˚C. Real-time PCR was performed using a real-time PCR thermocycler (Applied Biosystems, Foster City, CA, USA) and quantified using SYBR® Green PCR Master Mix (Applied Biosystems) using 1 μl cDNA in a final reaction volume of 20 μl. The PCR reactions were cycled 45 times after initial denaturation (94˚C, 1 min) with the following parameters: denaturation at 94˚C, 10 sec; annealing at 58˚C, 15 sec (caspase-3, caspase-8, GAPDH) at 60˚C, 10 sec (HO-1, caspase-9), and extension at 72˚C, 10 sec. At the end of PCR, the temperature was increased from 60 to 95˚C at a rate of 2˚C/min, and the fluorescence was measured every 15 sec to plot the melting curve. GAPDH was used as the internal control. SDS 2.2.1 software (Applied Biosystems) was used to perform relative quantification of the target genes using the ΔΔCt method. The primers (Takara Bio Inc., Dalian, China), shown in Table I, were designed using Primer Express 3.0 Software (Applied Biosystems).

Western blot analysis. Cells were washed three times with cold phosphate-buffered saline (PBS; 10 mmo/l HEPES, 140 mmo/l NaCl and 2.5 mmo/l $CaCl_2$, pH 7.4) and then lysed in Tris-buffered saline (TBS; 50 mmo/l Tris-HCl, pH 8.0, 150 mmo/l NaCl, 100 μg/ml phenylmethylsulfonyl fluoride and 1% Triton X-100) for 30 min on ice. Then the cells were divided into two Eppendorf tubes, one for cytoplasmic and mitochondrial protein extraction and the other one for total protein extraction following the manufacturer's instructions. Protein (60 mg) was fractioned by SDS-PAGE using 10% gels and was transferred electrophoretically to hydrophilic polyvinylidene fluoride membranes (GE Healthcare Life Sciences, Piscataway, NJ, USA). The membrane was blocked with 5% skimmed milk in TBS overnight and incubated with polyclonal antibodies of HO-1 (1:800), cleaved-caspase-3 (1:800), caspase-8 (1:800), caspase-9 (1:800), cleaved-PARP (1:800), caspase-12 (1:800), Cyto C (1:800) and β-actin (1:1,200) for 2 h, washed in TBS-T (0.1% Tween-20 in TBS) and incubated with secondary antibodies [anti-rabbit IgG (1:1,500) and anti-mouse IgG (1:1,500)] at room temperature for 1 h. The

Table I. Primer sequences of gene mRNA for real-time PCR.

Gene	Forward primer	Reverse primer	Product (bp)
HO-1	5'-ATGGCCTCCCTGTACCACATC-3'	5'-TGTTGCGCTCAATCTCCTCCT-3'	55
Caspase-3	5'-GACTCTGGAATATCCCTGGACAACA-3'	5'-AGGTTTGCTGCATCGACATCTG-3'	140
Caspase-8	5'-CAAGAGGAAATCTCCAAATGCAAC-3'	5'-CAGGATGTCCAACTTTCCTTCTCC-3'	108
Caspase-9	5'-GAGCAGTGGGCTCACTCTGAA-3'	5'-GGAAATTAAAGCAACCAGGCATC-3'	106
GAPDH	5'-GAAGGTGAAGGTCGGATGC-3'	5'-GAAGATGGTGATGGGATTTC-3'	226

signals were visualized by exposing the membrane to X-ray film (Carestream Health, Inc., Xiamen, China), and quantified using Image J 1.44p (National Institutes of Health, Bethesda, MD, USA).

FCM analysis
Apoptosis analysis. Cell death was determined using flow cytometric analysis, subsequent to the cells being double-stained with Annexin V-fluorescein isothiocyanate (FITC) and 7-aminoactinomycin D (7-AAD). The cells (10^5/sample) were incubated for 24 h after different treatments, and then they were harvested and washed twice with cold PBS. Cell pellets were harvested and resuspended with 500 μl of 50 mg/ml 7-AAD and Annexin V both/respectively containing RNase. After being stained at room temperature for 15 min in dark, the samples were analyzed by flow cytometry using the BD FACSCalibur™ flow cytometer with BD CellQuest™ software (Becton-Dickinson and Company, Franklin Lakes, NJ, USA). Parameters were confirmed by no-treated Kasumi-1 cells with Annexin V or 7-AAD staining, respectively, and data were collected in FL2 channel for Annexin V and FL3 channel for 7-AAD.

ROS generation. The measurement of intracellular ROS was based on the ROS-mediated conversion of non-fluorescent dichlorofluorescin diacetate (DCFH-DA) into DCFH. Briefly, after different treatments, cells were then centrifuged and resuspended in 1X PBS containing a final concentration of 10 μmol/l DCFH-DA (Beyotime) and incubated at 37˚C for 30 min. Cells were subsequently washed with 1X PBS and analyzed using the FL2 channel in a flow cytometer.

Intracellular calcium ion (Ca^{2+}) accumulation. Cells in culture medium were loaded with fluo-3/AM (final concentration, 10 μmol/l), an intracellular Ca^{2+} indicator (Dojindo), at 37˚C for 30 min. The cells were washed and resuspended in culture medium. Intracellular Ca^{2+} was measured using a flow cytometer. A stimulus was applied to the cells 1 min after measuring the fluorescence intensity of resting cells, then continuous recording was started again until another stimulus was applied.

Mitochondrial transmembrane potential (MTP) change. Cells were resuspended in 500 μl of JC-1 probe staining working solution (Beyotime), incubated at 37˚C for 20 min, and washed with JC-1 staining working solution (1X) three times. Thereafter FCM was used to detect the intensities of green and red fluorescences of JC-1 to determine the MTP changes. JC-1

showed an aggregation structure with red fluorescence and a monomer structure with green fluorescence when MTP was reduced. Since there existed inter-interference between green (JC-1) and GFP fluorescence in FL1 channel, the decrease of red fluorescence in FL2 channel was chosen to reflect the change of MTP in this study.

Statistical analysis. Data are expressed as mean ± standard deviation (mean ± SD). Analysis of variance (ANOVA) and Mann-Whitney test were performed with SPSS 16.0 (SPSS, Inc., Chicago, IL, USA). A value of $P<0.05$ was considered to indicate a statistically significant difference.

Results

Transfection of Kasumi-1 cells with recombined lentivirus of HO-1 siRNA (pRNAi-siHO-1-GFP). After transfection for 24, 48 and 72 h, the GFP expression in Kasumi-1 cells was observed using a fluorescence microscopy. The efficiency of transfection (average proportion of GFP-expressing cells to the total cell count) was >80% after transfection for 72 h (Fig. 1A). FCM analysis showed that the transfection efficiency rose to 73.70% at 48 h and peaked at 72 h (Fig. 1B). Then the cells were harvested after transfection for 72 h to detect expression of mRNA and protein of HO-1 by real-time PCR and western blot analysis. The rates of silenced HO-1 mRNA and protein expression were 77.95 and 75.95%, respectively (Fig. 1C and D).

Targeted HO-1 silencing enhanced the chemotherapy sensitivity of Kasumi-1 cells to DNR. The inhibitory effects of various concentrations of DNR (5, 7.5, 10 and 12.5 μg/ml) on Kasumi-1 cell growth for different time intervals (24, 48 and 72 h) were investigated. DNR exerted moderate inhibitory effects on cell proliferation in a time- and dose-dependent manner (Fig. 2A). IC_{50} (the concentration necessary to produce 50% inhibition of cell growth) value of DNR was 7.0 μg/ml. Using Kasumi-1 cells alone and Kasumi-1 cells with vehicle treatment as the control, the cells were exposed to DNR (7.0 μg/ml) and pRNAi-siHO-1-GFP alone or together for 24, 48 and 72 h. The inhibition rate of Kasumi-1 cells with HO-1 siRNA plus DNR treatment was significantly higher than that with HO-1 siRNA or DNR treatment alone (Fig. 2B). Besides, HO-1 siRNA and vehicle itself did not obviously affect the survival of Kasumi-1 cells.

Caspase activation is related to Kasumi-1 cell apoptosis mediated by pRNAi-siHO-1-GFP. To further identify the
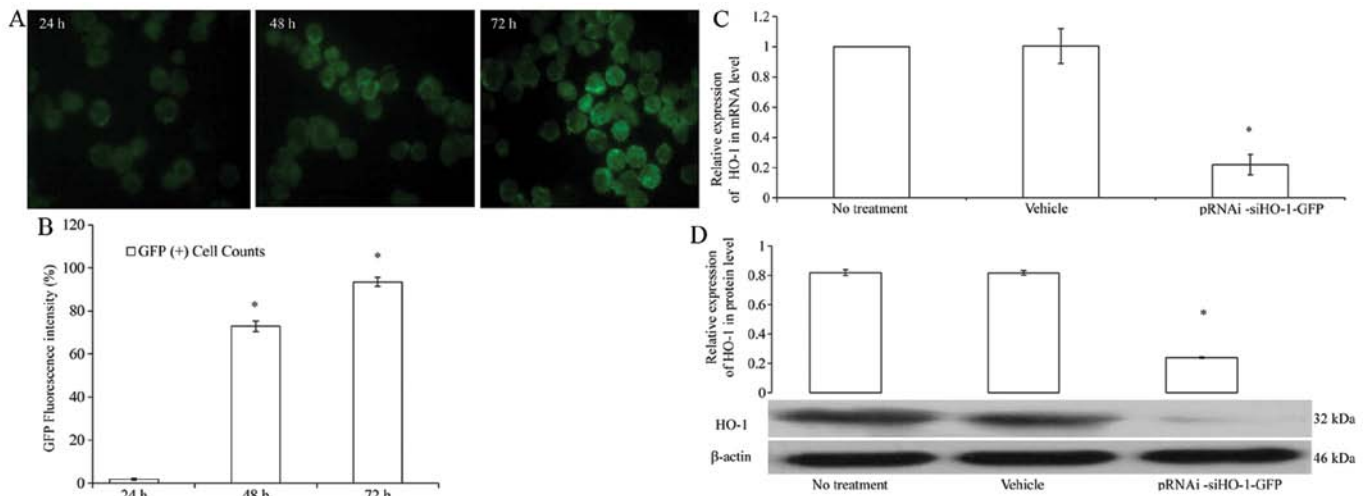
Figure 1. Transfection of Kasumi-1 cells with recombined lentivirus vector carrying HO-1 siRNA. (A) Transfection efficiency of Kasumi-1 cells was observed by a fluorescence microscope. In fluorescent field, the transfection efficiency exceeded 80% after 72 h. (B) GFP expression was detected by FCM. The transfection efficiency was 1.51, 73.70 and 95.87% after 24, 48 and 72 h respectively, showing time-dependency (*p<0.05). (C) Kasumi-1 cells transfected by pRNAi-GFP or pRNAi-siHO-1-GFP were harvested to detect mRNA expression of HO-1 after 72 h. HO-1 expression was significantly reduced in Kasumi-1 cells transfected by pRNAi-siHO-1-GFP (*p<0.05). (D) Cells were collected in the same way as that described (C). The protein expression of HO-1 was detected by western blot analysis. The expression of HO-1 protein was significantly downregulated (*p<0.05). Relative expression levels of HO-1 mRNA and protein are presented as (mean ± SD) from three independent experiments.
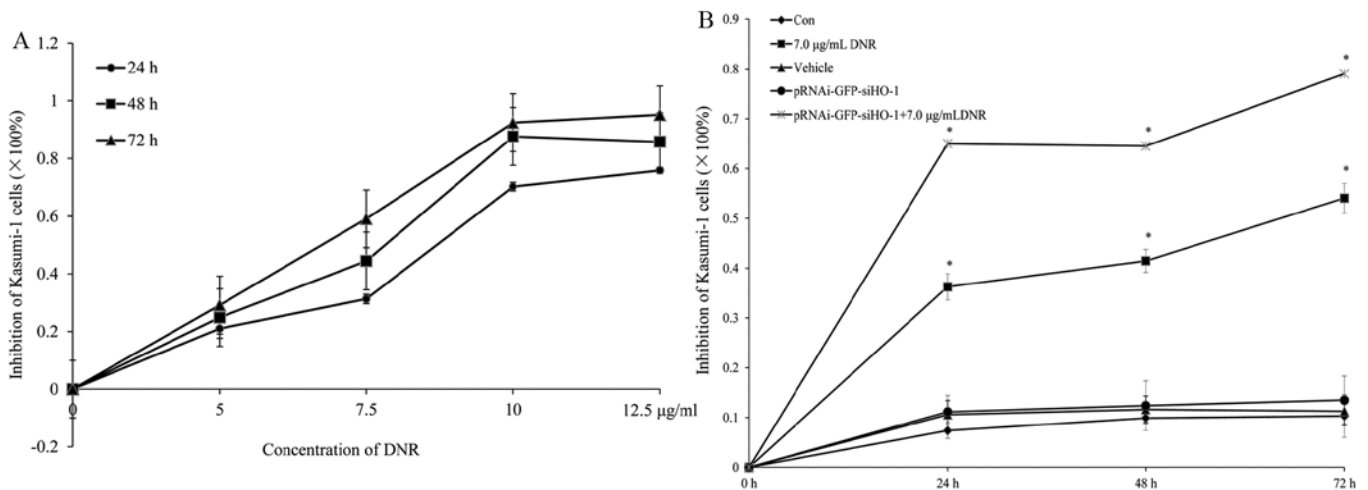

Figure 2. Effects of DNR and HO-1 siRNA treatment alone or together on the survival of Kasumi-1 cells. (A) The growth inhibitory rate of Kasumi-1 cells treated with DNR at indicated concentrations (0, 5, 7.5, 10 and 12.5 µg/ml) for 24, 48 and 72 h were time- and dose-dependent. (B) The inhibition rate of Kasumi-1 cells with HO-1 siRNA plus DNR treatment was significantly higher than that with HO-1 siRNA or DNR treatment alone (*p<0.05).

inhibitory effect of DNR on Kasumi-1 cells, FCM was used to detect the apoptotic rate after the cells were treated as mentioned above for 24 h (Fig. 3A and B). The apoptotic rate of DNR treatment alone was (39.66±1.66)%, while it increased to (75.42±1.79)% together with pRNAi-siHO-1-GFP, which was significantly higher than those of Kasumi-1 cell group, vehicle group and pRNAi-siHO-1-GFP group [(8.45±0.89)%, (9.88±0.50)% and (9.80±0.81)% respectively]. MTT assay further confirmed that pRNAi-siHO-1-GFP or vehicle alone did not induce apoptosis, so the possibilities that pRNAi-siHO-1-GFP or vehicle led to cell death were excluded. At the same time, the cells after DNR (7.0 µg/ml) treatment only or that combined with pRNAi-siHO-1-GFP were collected. Real-time

PCR and western blot analysis were used to detect the mRNA and protein expressions of caspase-3 (cleaved-caspase-3), caspase-8 and caspase-9, which were 11.4-, 5.5- and 8.2-fold compared with those of DNR treatment only, respectively (Fig. 3C-E), suggesting that HO-1 siRNA promoted apoptosis through caspase activation.

Protein expressions of HO-1, cleaved-caspase-3, caspase-8 and caspase-9. In order to further discuss the role of HO-1 siRNA in enhancing apoptosis through caspases activation, various concentrations (5, 7.5, 10 and 12.5 µg/ml) of DNR were used to treat Kasumi-1 cells with/without pRNAi-siHO-1-GFP transfection. Western blot analysis was used
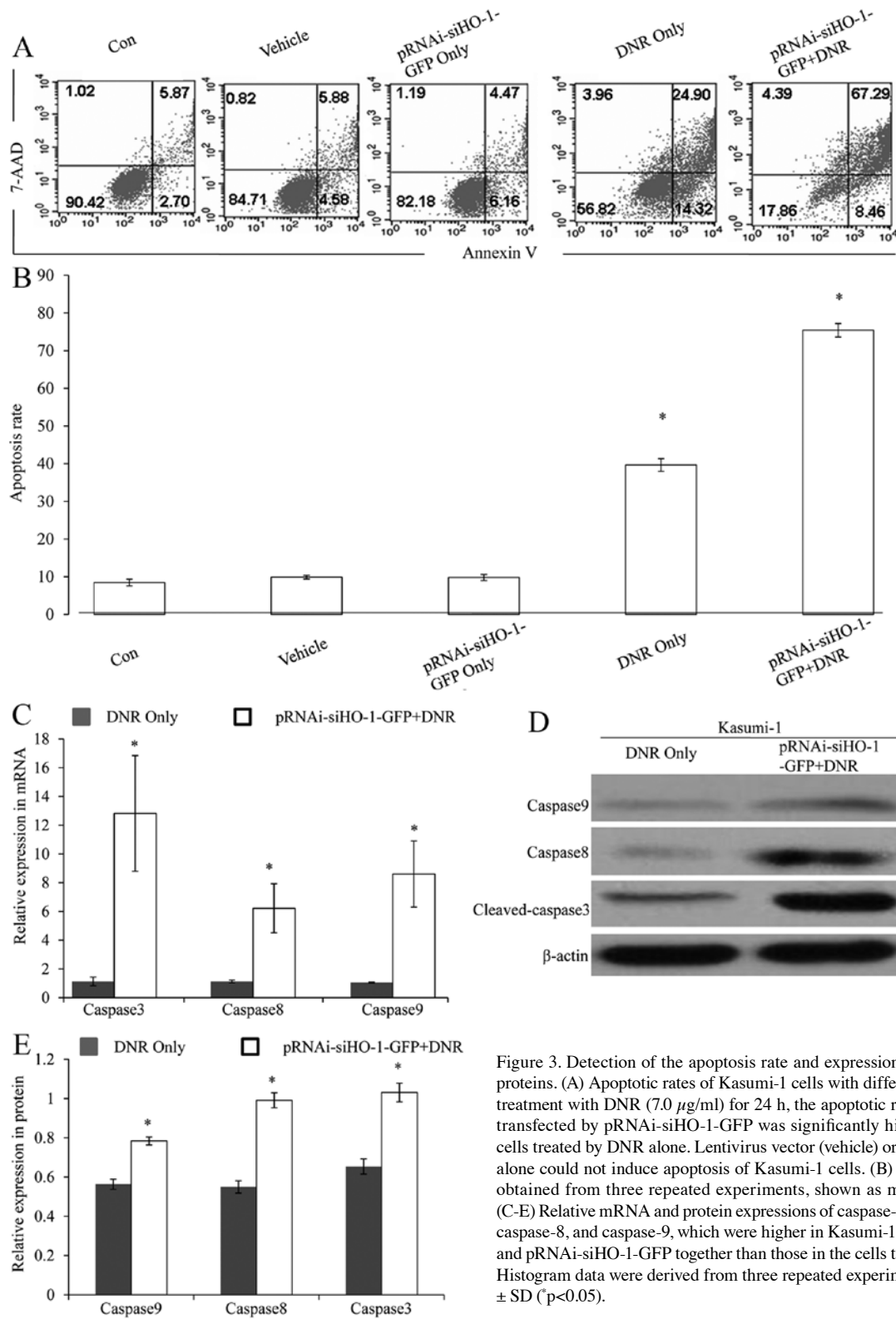
Figure 3. Detection of the apoptosis rate and expression of apoptosis-related proteins. (A) Apoptotic rates of Kasumi-1 cells with different treatments. After treatment with DNR (7.0 μg/ml) for 24 h, the apoptotic rate of Kasumi-1 cells transfected by pRNAi-siHO-1-GFP was significantly higher than that of the cells treated by DNR alone. Lentivirus vector (vehicle) or pRNAi-siHO-1-GFP alone could not induce apoptosis of Kasumi-1 cells. (B) Histogram data were obtained from three repeated experiments, shown as mean ± SD (*p<0.05). (C-E) Relative mRNA and protein expressions of caspase-3 (cleaved-caspase-3), caspase-8, and caspase-9, which were higher in Kasumi-1 cells treated by DNR and pRNAi-siHO-1-GFP together than those in the cells treated by DNR alone. Histogram data were derived from three repeated experiments, shown as mean ± SD (*p<0.05).

to detect the expressions of HO-1 and apoptosis-related genes (cleaved-caspase-3, caspase-8 and caspase-9). Protein expressions of cleaved-caspase-3, caspase-8 and caspase-9 increased with rising concentration of DNR dose-dependently. After combined pRNAi-siHO-1-GFP and DNR treatment, the protein expression of HO-1 was lower than that of DNR treatment alone (Fig. 4A), while the expressions of apoptosis-related proteins were higher (Fig. 4C-E). Therefore, HO-1 siRNA was able to facilitate cell apoptosis through activation of caspase activation.

Caspase-12, Cytoplasm-Cyto C and cleaved-PARP are involved in apoptosis mediated by HO-1 siRNA. To further discuss the possible mechanisms involved in the activation
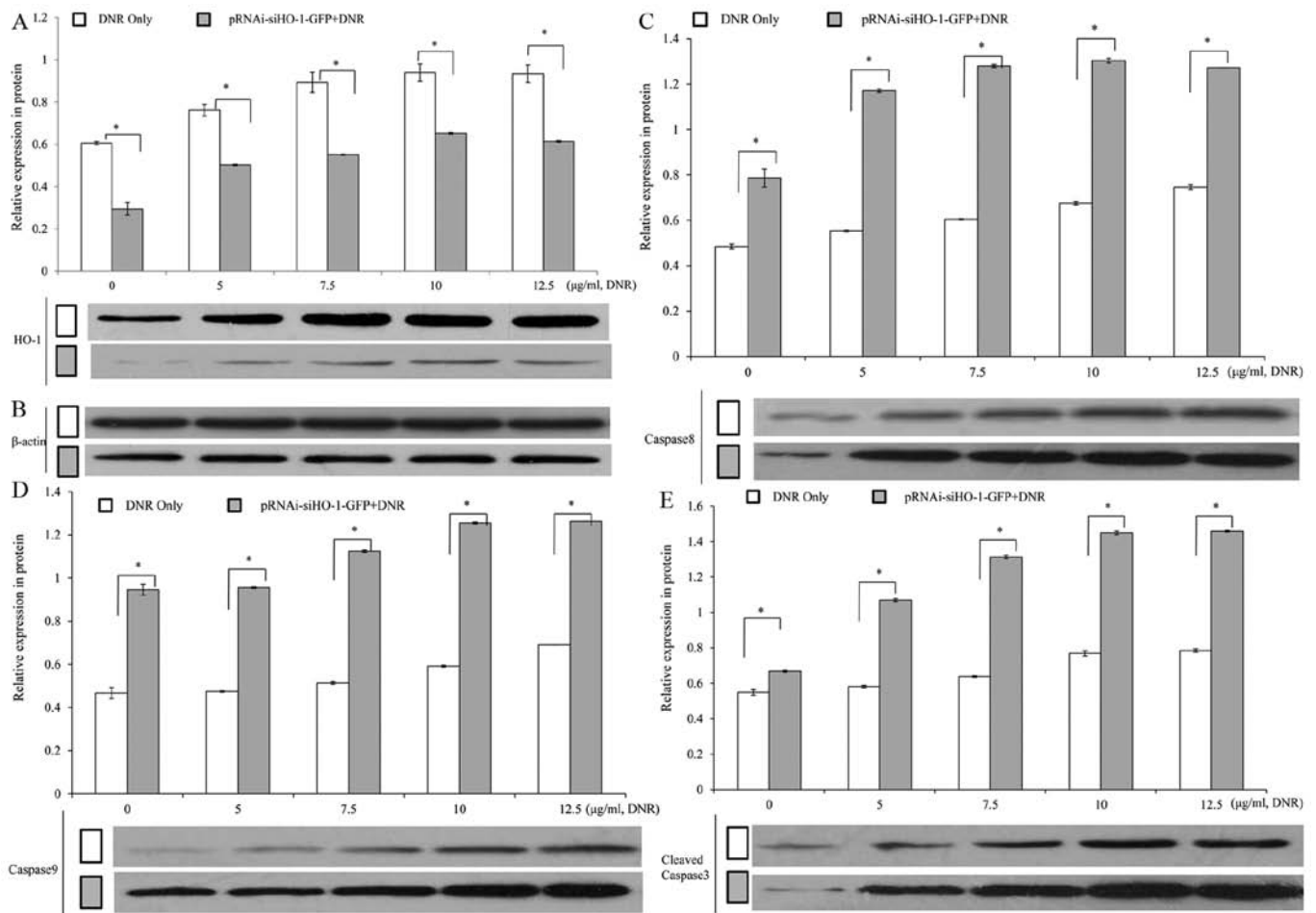
Figure 4. Changes in HO-1 and apoptosis-related protein expression induced by DNR. (A) Protein expression of HO-1 was significantly inhibited in Kasumi-1 cells transfected by pRNAi-siHO-1-GFP, which was induced by DNR treatment in a dose-dependent manner and reached maximum at 10 μg/ml. Histogram represents the optical densities of HO-1 normalized to that of β-actin (B). The data were derived from three repeated experiments (mean ± SD, *p<0.05). (B) The expressions of β-actin were uniform in Kasumi-1 cells and those transfected by pRNAi-siHO-1-GFP. (C-E) Protein expressions of caspase-8, caspase-9 and cleaved-caspase-3 increased with rising concentration of DNR dose-dependently, which reached maximum at 10 μg/ml. Histogram represents the optical densities of caspase-8, caspase-9 and cleaved-caspase-3 ratio normalized to that of β-actin. Expression of caspase-8, caspase-9 and cleaved-caspase-3 in Kasumi-1 cells treated by HO-1 siRNA together with DNR were significantly higher than those in the cells treated by DNR alone. The data were derived from three repeated experiments (mean ± SD, *p<0.05).

of cleaved-caspase-3, caspase-8 and caspase-9, two classical pathways, i.e., endoplasmic reticulum apoptotic pathway and mitochondrial apoptotic pathway, were taken into consideration. Caspase-12, a characteristic protein mediating the endoplasmic reticulum apoptotic pathway, as well as Cyto C which was activated and released from mitochondria into cytoplasm in the mitochondrial apoptotic pathway. Nuclear poly(ADP-ribose) polymerase (PARP) is one of the main cleavage targets of caspase-3. Cleavage of PARP facilitates cellular disassembly as a marker of cell apoptosis. In this study, western blot analysis was used to determine the protein expression of caspase-12, cytoplasm-Cyto C and cleaved-PARP after treatment with 7.0 μg/ml DNR with/without HO-1 siRNA. The results indicated that HO-1 siRNA could promote the expression of caspase-12, cytoplasm-Cyto C and cleaved-PARP (Fig. 5) in Kasumi-1 cells when treated with DNR.

HO-1 siRNA increases the intracellular Ca²⁺ accumulation in Kasumi-1 cells. Ca²⁺ homeostasis is mainly maintained through endoplasmic reticulum to which most Ca²⁺ activities

are related. The changes of intracellular [Ca²⁺] give rise to endoplasmic reticulum stress, while over-stress may lead to cell apoptosis (16). In addition, Ca²⁺ is also a key link of endoplasmic reticulum and mitochondrial function. Considerable Ca²⁺ releases due to endoplasmic reticulum stress are bound to be absorbed by mitochondria because of membrane potential gradient, and mitochondrial calcium overload is one of the known important apoptosis-inducing factors. On endoplasmic reticulum, the release of Ca²⁺ enhances the sensitivity of mitochondria, which changes the permeability and depolarizes mitochondrial membrane, thus resulting in cell apoptosis (17,18). Therefore, the activations of endoplasmic reticulum and mitochondrial apoptotic pathways can be reflected by intracellular Ca²⁺ concentration. Fluo3-AM is a fluorescent dye that can penetrate the cell membrane and can be cleaved in Fluo 3 form by esterase. Fluo 3 in combination with calcium ions can generate strong and detectable fluorescence. In this study, Fluo3-AM probe was used to detect Ca²⁺ accumulation of Kasumi-1 cells after different treatments. After combined treatment with pRNAi-GFP-siHO-1 and DNR (7.0 μg/ml)
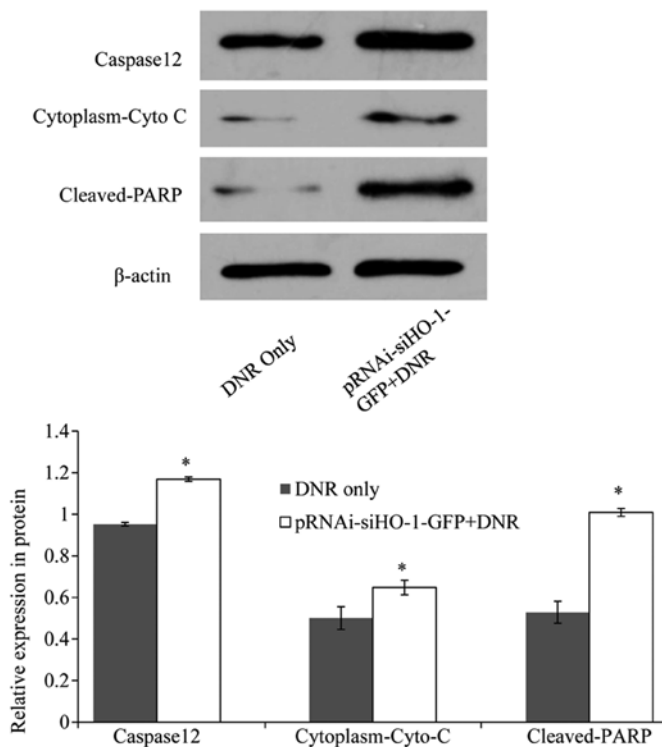
Figure 5. Caspase-12 activation, Cyto C release and PARP cleavage were mediated by pRNAi-siHO-1-GFP. After treatment with pRNAi-siHO-1-GFP and DNR, the expression of caspase-12, cytoplasm-Cyto C and cleaved-PARP was significantly higher than those in Kasumi-1 cells treated by DNR alone. Histogram represents the optical densities of caspase-12, Cyto C and cleaved-PARP normalized to β-actin. The data were obtained from three repeated experiments (mean ± SD, $^*p<0.05$).

between intracellular Ca^{2+} accumulation and ROS generation, and the latter often precedes the former. On one hand, intracellular ROS production can activate the mitochondrial apoptotic pathway and augment the accumulation of intracellular Ca^{2+} simultaneously. On the other hand, the accumulation of intracellular Ca^{2+} can activate multiple signal pathways as a second messenger, thus increasing the generation of ROS. Excessive ROS leads to cell oxidative damage, thus promoting cell apoptosis (19,20). In our study, the increase of cytoplasmic Cyto C suggested that HO-1 siRNA facilitated cell apoptosis through the mitochondrial apoptotic pathway. To further explore the relationship between ROS generation and HO-1 siRNA-mediated cell apoptosis, DCFH-DA probe was used to detect the intracellular ROS generation of Kasumi-1 cells after different treatments. After combined treatment with pRNAi-GFP-siHO-1 and DNR (7.0 µg/ml) for 24 h, the ROS generation was higher than those of other groups (Fig. 7A). Besides, ROS generation in Kasumi-1 cells increased with prolonged infection with pRNAi-siHO-1-GFP and peaked at 24 h (21.90%) (Fig. 7B).

MTP changes detected by FCM. In this study, intracellular Ca^{2+} accumulation and ROS generation were involved in cell apoptosis mediated by HO-1 siRNA. Accumulation of these two substances might open the mitochondrial permeability transition pore (MPTP) (21), which reduced MTP and subsequently activated pro-apoptotic genes, thus inducing cell apoptosis (22). Reduction of MTP is an early event in activation of the mitochondrial apoptotic pathway (23). In order to evaluate the changes of MTP in HO-1 siRNA-mediated cell apoptosis, JC-1 probe was used to detect the green and red fluorescence intensities in Kasumi-1 cells. Compared with other groups, red fluorescence remarkably decreased in the group treated by DNR (7.0 µg/ml) together with pRNAi-siHO-1-GFP (p<0.05) (Table II and Fig. 8).

Intensity of red fluorescence was significantly lower in cells transfected by pRNAi-siHO-1-GFP and treated by DNR together than those in the cells undergoing pRNAi-siHO-1-GFP or DNR treatment alone.
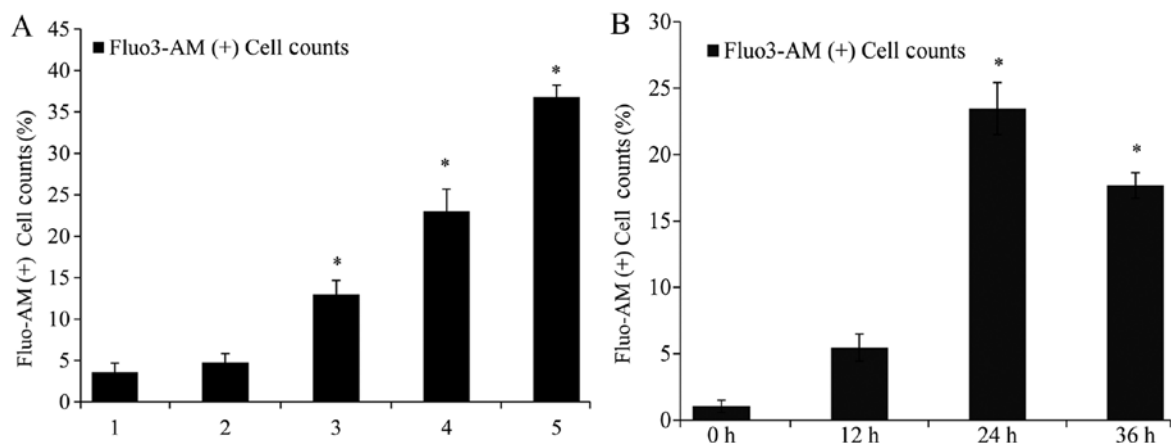
for 24 h, the intracellular Ca^{2+} accumulation was higher than those of the other groups (Fig. 6A). Besides, Ca^{2+} accumulation in Kasumi-1 cells increased with prolonged infection with pRNAi-siHO-1-GFP and peaked at 24 h (23.38%) (Fig. 6B).

HO-1 siRNA increased the generation of ROS in Kasumi-1 cells. During cell apoptosis, there is also a close relationship

Figure 6. Intracellular Ca^{2+} accumulation detected by FCM. (A) Intracellular Ca^{2+} accumulation of cells after different treatments. 1, Control group (Kasumi-1 cells), 3.77%. 2, Vehicle, 5.89%. 3, Treated by DNR (7.0 µg/ml) alone for 24 h, 14.88%. 4, Infected by pRNAi-siHO-1-GFP for 24 h, 25.92%. 5, Treated by DNR (7.0 µg/ml) and pRNAi-siHO-1-GFP together for 24 h, 36.02%; $^*p<0.05$. (B) Intracellular Ca^{2+} accumulation of Kasumi-1 cells infected by pRNAi-siHO-1-GFP at different time-points. 1, Con (0 h); 2, 12 h; 3, 24 h; 4, 36 h. Ca^{2+} accumulation was time-dependent reaching the maximal level at 24 h (23.38%); $^*p<0.05$.
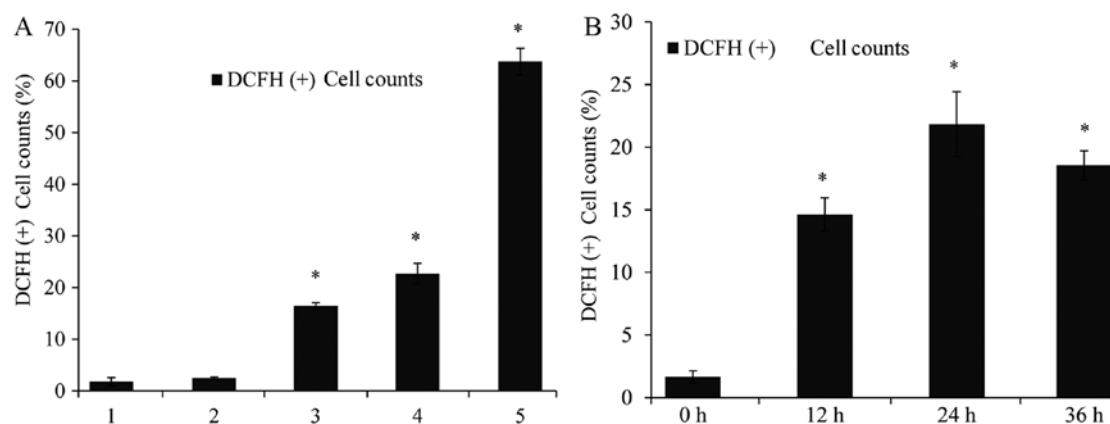
Figure 7. Intracellular ROS generation analyzed by FCM. (A) ROS generation of cells after different treatments. 1, Control group (Kasumi-1 cells), 1.21%. 2, Vehicle, 2.43%. 3, Treated by DNR (7.0 µg/ml) alone for 24 h, 16.51%. 4, Infected by pRNAi-siHO-1-GFP for 24 h, 23.16%. 5, Treated by DNR (7.0 µg/ml) and pRNAi-siHO-1-GFP together for 24 h, 64.73%; *p<0.05. (B) Intracellular ROS generation of Kasumi-1 cells infected by pRNAi-siHO-1-GFP at different time-points. 1, Con (0 h); 2, 12 h; 3, 24 h; 4, 36 h. ROS generation was time-dependent reaching the maximal level at 24 h (21.90%); *p<0.05.

Table II. Red fluorescence intensity of JC-1 in Kasumi-1 cells with indicated treatments determined by FCM.

	No treatment	Vehicle only	pRNAi-siHO-1-GFP only	DNR only	pRNAi-siHO-1-GFP + DNR
Fluorescence intensity (red)	357.30	353.01	303.74	283.97	190.08

Relationship between endoplasmic reticulum and mito-chondrial apoptotic pathways in HO-1 siRNA-mediated apoptosis. HO-1 siRNA contributed to cell apoptosis through endoplasmic reticulum and mitochondrial apoptotic pathways. Activation of caspase-12 and Ca^{2+} accumulation were involved in the endoplasmic reticulum apoptotic pathway, while ROS generation, reduction of MTP and release of Cyto C were involved in activation of the mitochondrial apoptotic pathway. To elucidate the relationship between the two pathways in cell apoptosis mediated by HO-1 siRNA, antioxidant NAC or (and) Ca^{2+}-chelating agent BAPTA-AM were used alone or in combination to pretreat Kasumi-1 cells infected by pRNAi-siHO-1-GFP, and then DNR (7.0 µg/ml) was added. Subsequently, Ca^{2+} accumulation, ROS generation and cell apoptosis were detected by FCM. Meanwhile, the protein expressions of caspase-12 and cytoplasm-Cyto C were deter-mined by western blot analysis to discuss the influences of inhibited ROS generation or (and) Ca^{2+} accumulation on the endoplasmic reticulum and mitochondrial apoptotic pathways.
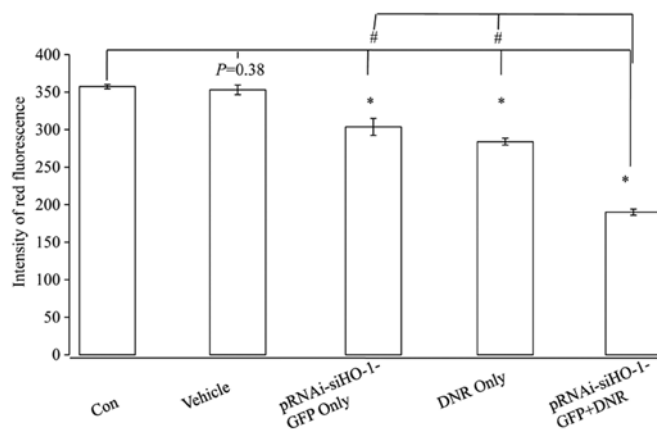

Figure 8. Intensity of the red fluorescence was determined by FCM. Data shown in histogram were derived from three repeated experiments (mean ± SD, *,#p<0.05).

NAC or (and) BAPTA-AM inhibits caspase-12 expression and Cyto C release mediated by HO-1 siRNA. To further clarify the relationship between endoplasmic reticulum and mitochondrial apoptotic pathways in HO-1 siRNA-mediated apoptosis, Kasumi-1 cells were treated as follows: 1, Kasumi-1 cells were treated by DNR (7.0 µg/ml) alone (control group). 2, Kasumi-1 cells were treated with pRNAi-siHO-1-GFP plus DNR (7.0 µg/ml). 3, After pretreatment with 10 mmol/l NAC, Kasumi-1 cells were treated with pRNAi-siHO-1-GFP plus DNR (7.0 µg/ml). 4, After pretreatment with 10 µmol/l BAPTA-AM, Kasumi-1 cells were treated with pRNAi-siHO-1-GFP plus DNR (7.0 µg/ml). 5, After combined

pretreatment with 10 µmol/l BAPTA-AM and 10 mmo/l NAC, Kasumi-1 cells were treated with pRNAi-siHO-1-GFP plus DNR (7.0 µg/ml). The protein expression of caspase-12 and cytoplasmic Cyto C after different treatments was detected by western blot analysis. The protein expressions of caspase-12 and cytoplasmic Cyto C were significantly reduced in Kasumi-1 cells pretreated with NAC or (and) BAPTA-AM than those of other groups (p<0.05) (Fig. 9).

NAC or (and) BAPTA-AM restrains the Ca^{2+} accumulation and ROS generation mediated by HO-1 siRNA. In order to further explore the relationship between Ca^{2+} accumulation
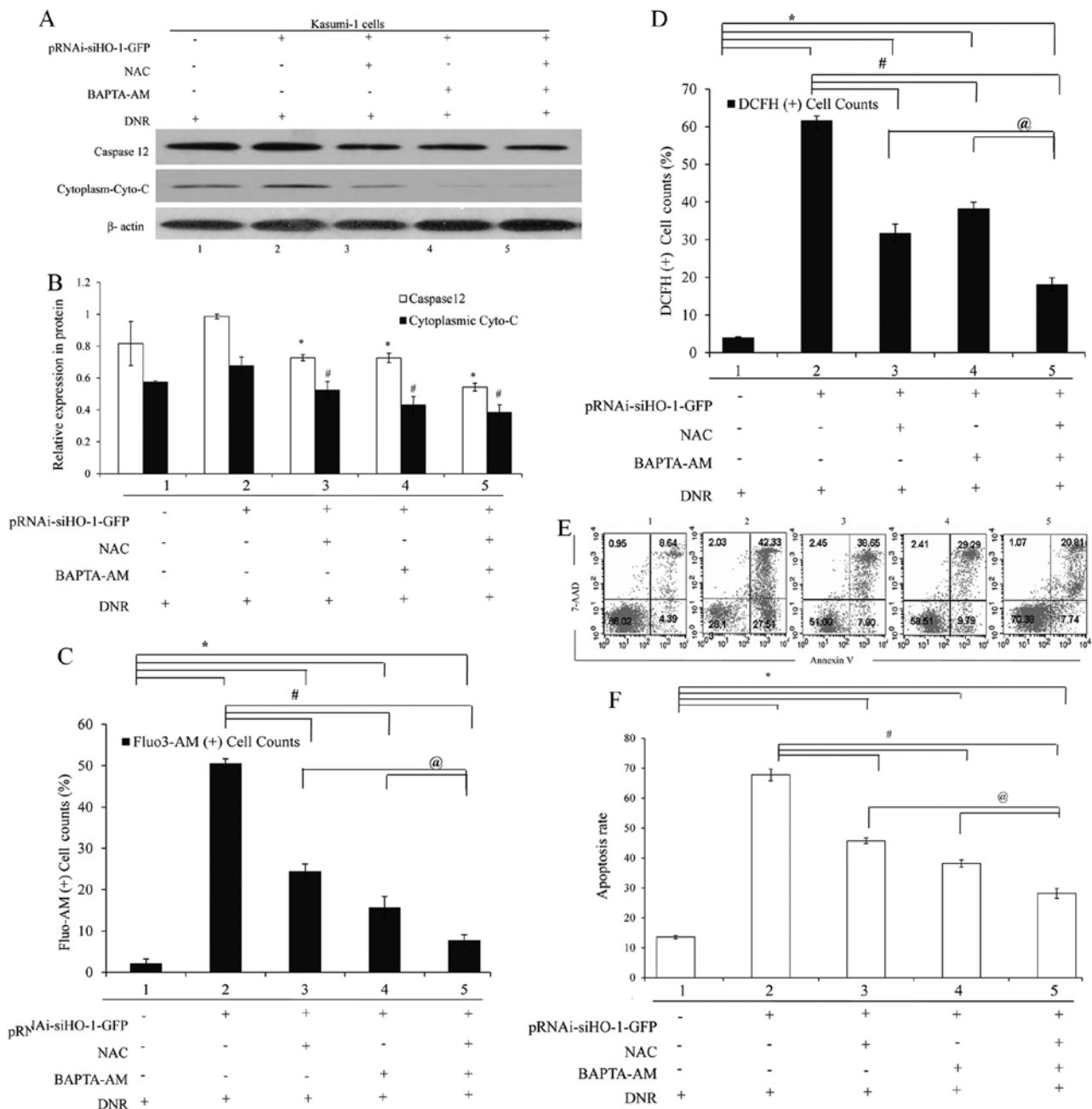
Figure 9. (A) Expression of caspase-12 and cytoplasm-Cyto C was reduced by NAC or (and) BAPTA-AM treatment. Protein expression of caspase-12 and cytoplasm-Cyto C in Kasumi-1 cells was detected by western blot analysis (+ represents treatment, while - represents without treatment). Expression of caspase-12 and cytoplasm-Cyto C protein of cells that was pretreated by 10 mmol/l NAC or (and) 10 µg/ml BAPTA-AM before infection with pRNAi-siHO-1-GFP and then treated with 7.0 µg/ml DNR were more significantly inhibited than those of other groups (*p<0.05). 1, Kasumi-1 cells were treated by DNR (7.0 µg/ml) alone (control group). 2, Kasumi-1 cells were treated with pRNAi-siHO-1-GFP plus DNR (7.0 µg/ml). 3, After pretreatment of 10 mmol/l NAC, Kasumi-1 cells were treated with pRNAi-siHO-1-GFP plus DNR (7.0 µg/ml). 4, After pretreatment of 10 µmol/l BAPTA-AM, Kasumi-1 cells were treated with pRNAi-siHO-1-GFP plus DNR (7.0 µg/ml). 5, After combined pretreatment of 10 µmol/l BAPTA-AM with 10 mmol/l NAC, Kasumi-1 cells were treated with pRNAi-siHO-1-GFP plus DNR (7.0 µg/ml). (B) Histogram represents the optical densities of caspase-12 and cytoplasm-Cyto C normalized to that of β-actin. Data were obtained from three repeated experiments (mean ± SD, *,#p<0.05). (C) Intracellular Ca2+ accumulation decreased after treatment by NAC or (and) BAPTA-AM. Ca2+ accumulation in Kasumi-1 cells transfected with pRNAi-siHO-1-GFP and treated by DNR was the highest (52.56%), while Ca2+ accumulations reduced because of NAC or BAPTA-AM pretreatment before pRNAi-siHO-1-GFP and DNR treatment (24.83 and 14.37%, respectively). After pretreatment with NAC and BAPTA-AM together, intracellular Ca2+ accumulation was the lowest (7.72%). All data were derived from three repeated experiments (mean ± SD). Compared with the control group, *p<0.05. Compared with group 2, #p<0.05. Compared with group 3 or 4, @p<0.05. Groups 1-5 are represented as mentioned above (A). (D) Intracellular ROS generation was inhibited by the treatment of NAC or (and) BAPTA-AM. ROS generation in Kasumi-1 cells transfected with pRNAi-siHO-1-GFP and treated by DNR was the highest (62.73%), while ROS generations reduced because of NAC or BAPTA-AM pretreatment before pRNAi-siHO-1-GFP and DNR treatment (32.37 and 39.87%, respectively). After pretreatment with NAC and BAPTA-AM together, ROS generation was the lowest (18.01%). All data were derived from three repeated experiments (mean ± SD). Compared with the control group, *p<0.05. Compared with group 2, #p<0.05. Compared with group 3 or 4, @p<0.05. Groups 1-5 are represented as mentioned above (A). (E) NAC or (and) BAPTA-AM reduced cell apoptosis mediated by HO-1 siRNA. Apoptotic rate of Kasumi-1 cells transfected with pRNAi-siHO-1-GFP and treated by DNR was the highest (69.84%), while apoptotic rates reduced because of NAC or BAPTA-AM pretreatment before pRNAi-siHO-1-GFP and DNR treatment (46.55 and 39.08% respectively). After pretreatment with NAC and BAPTA-AM together, cell apoptosis was suppressed significantly (28.55%). 1-5, Groups are represented as mentioned above (A). (F) Cell apoptotic rate is represented by a histogram. All data were derived from three repeated experiments (mean ± SD). Compared with the control group, *p<0.05. Compared with group 2, #p<0.05. Compared with group 3 or 4, @p<0.05. Groups 1-5 are presented as mentioned above (A).
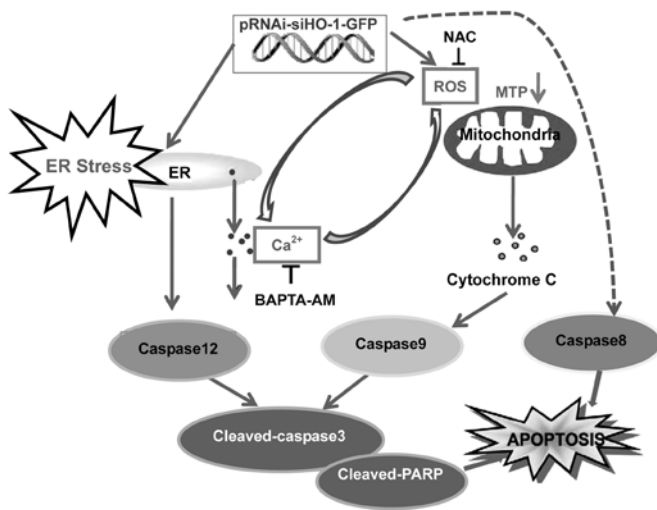
Figure 10. Schematic diagram showing how pRNAi-siHO-1-GFP mediated apoptosis in Kasumi-1 cells. Endoplasmic reticulum apoptotic pathway. Endoplasmic reticulum stress was caused in Kasumi-1 cells infected with pRNAi-siHO-1-GFP, which released Ca²⁺ and further activated caspase-12 to affect cell apoptosis in cooperation with ROS generated by the mitochondrial respiratory chain. Caspase-12 enabled apoptosis by boosting the cleaving function of caspase-3. Mitochondrial apoptotic pathway. The expression of HO-1 was downregulated in Kasumi-1 cells infected with pRNAi-siHO-1-GFP, and the resistance to oxidative stress was weakened, which increased ROS generation as well as membrane pore permeability. Then MTP was decreased and Cyto C was released from mitochondria to cytoplasm. The changes further activated caspase-9 and caspase-3 (cleaved-caspase-3), and then activated the PARP cleavage and proteolysis. In summary, ROS generation and Ca²⁺ accumulation interacted in the cell apoptosis mediated by HO-1 siRNA. In addition, the Fas-FasL pathway could cascade-activate caspase-8 and effector protein cleaved-caspase-3 to induce cell apoptosis. However, the detailed approach still requires in-depth studies.

and ROS generation in cell apoptosis mediated by HO-1 siRNA, Kasumi-1 cells were treated as described above. Intracellular Ca²⁺ accumulation and ROS generation after different treatments were detected by FCM to unravel the relationship between them in Kasumi-1 cell apoptosis mediated by HO-1 siRNA. The control group was used to confirm the analysis parameters of FL2 channel on FCM. Both NAC and BAPTA-AM could effectively restrain the increases of intracellular Ca²⁺ and ROS caused by HO-1 siRNA (Fig. 9C and D).

NAC or (and) BAPTA-AM reduced cell apoptosis mediated by HO-1 siRNA. In order to confirm the influences of Ca²⁺ accumulation and ROS generation on the cell apoptosis mediated by HO-1 siRNA, apoptotic analysis was performed after cells were treated as described above. NAC and BAPTA-AM significantly alleviated HO-1 siRNA-mediated apoptosis (p<0.05) (Fig. 9E and F). Therefore, there may be potential Ca²⁺-ROS-interaction between endoplasmic reticulum and mitochondrial apoptotic pathways mediated by HO-1 siRNA to regulate cell apoptosis.

Discussion

In this study, the expression of HO-1 was successfully silenced by pRNAi-siHO-1-GFP. The transfection efficiency was 95.78% after 72 h. Real-time PCR and western blot analysis

showed that the silence rate of HO-1 reached >75%, which met the requirements of subsequent experiments.

DNR inhibited the proliferation of Kasumi-1 cells in a dose- and time-dependent manner, and pRNAi-siHO-1-GFP remarkably inhibited the survival of Kasumi-1 cells when exposure to the same dose of DNR. Besides, the apoptotic rate of Kasumi-1 cells treated with DNR together with pRNAi-siHO-1-GFP was significantly higher than those of DNR group, pRNAi-siHO-1-GFP group and lentivirus vector (vehicle) group.

Therefore, HO-1 siRNA inhibited cell survival and facilitated cell apoptosis by augmenting the sensitivity to DNR. Similar results on HO-1 expression and CML have already been reported by our group (12-14). The results above provided theoretical basis for clinical practice to reverse DNR resistance and to overcome drug resistance in AML treatment. In addition, as evidenced by MTT assay and apoptosis detection, the lentivirus vector (vehicle) and HO-1 siRNA alone had no direct or specific effect on cell survival or apoptosis.

Cell apoptosis, the process of programmed cell death, predominantly maintains homeostasis. Inducing tumor cell apoptosis is one of the main strategies for tumor therapy. Apoptosis is closely related with the activation of caspase cascade. Activation of apoptotic protease, caspase, was able to activate effector cleaved-caspase-3, and degrade intracellular structural protein and functional protein, thus eventually leading to cell apoptosis (24). To investigate whether downregulation of HO-1 was conducive to cell apoptosis through caspase activation, western blot analysis was used to detect the expressions of cleaved-caspase-3, caspase-8 and caspase-9, which were obviously higher after DNR treatment together with pRNAi-siHO-1-GFP than the group treated with DNR alone. In subsequent experiments, Kasumi-1 cells and pRNAi-siHO-1-Kasumi cells were treated by different concentrations of DNR (5, 7.5, 10 and 12.5 µg/ml), and the expressions of these three apoptotic proteases were evidently higher in pRNAi-siHO-1-Kasumi cells. Accordingly, HO-1 siRNA was able to promote cell apoptosis by activating caspase cascade. The expression of HO-1 increased in a dose-dependent manner, probably because HO-1, as an acute phase protein HSP32, can be induced to be expressed under various stresses (25).

Moreover, whether two classical caspase-dependent apoptotic pathways (endoplasmic reticulum apoptotic pathway and mitochondrial apoptotic pathway) were involved in the cell apoptosis mediated by HO-1 siRNA was investigated preliminarily. Expressions of caspase-12, cytoplasm-Cyto C and cleaved-PARP were significantly higher in Kasumi-1 cells treated by HO-1 siRNA together with DNR than those of Kasumi-1 cells treated with DNR alone. Hence, the two classical caspase-dependent apoptotic pathways were involved in the Kasumi-1 cell apoptosis mediated by HO-1 siRNA.

Endoplasmic reticulum is an important calcium store for cells. A variety of incentives affect the Ca²⁺ steady state, which determines cell fate by giving rise to rapid or lasting changes (26). Ca²⁺ is also a crucial regulatory factor in endoplasmic reticulum and mitochondrial apoptotic pathways, whose accumulation activates the specific apoptotic protease caspase-12 in the former apoptotic pathway (27). Since HO-1 is located in the endoplasmic reticulum (28), HO-1 siRNA is capable

of releasing and accumulating Ca^{2+} by causing endoplasmic reticulum stress. In this study, once Kasumi-1 cells were infected with pRNAi-siHO-1-GFP, DNR could significantly increase intracellular Ca^{2+} accumulation. Ca^{2+} accumulation activated caspase-12 and further enhanced the cleaving action of caspase-3 to promote cell apoptosis. Ca^{2+} accumulation opened MPTP and reduced MTP, thus initiating the mitochondrial apoptotic pathway (29).

As one of the most important oxidation regulator enzymes, HO-1 can reduce the oxidation level to protect cells from damage (4). The expression of HO-1 was downregulated by HO-1 siRNA, which thereby destroyed the steady state of oxidation-reduction system and increased ROS generation. ROS may inhibit cell viability from three aspects. First, excessive ROS generation triggers cell death directly (30). Second, accumulation of ROS results in cell death by damaging the mitochondrial respiratory chain. Third, ROS can affect MTP that plays a critical role in maintaining mitochondrial oxidative phosphorylation, producing ATP and keeping cell physiological functions. The decline or loss of MTP is the main biological event in the mitochondrial apoptotic pathway (31). Furthermore, ROS generation activates the mitochondrial apoptotic pathway by reducing MTP, while release of Cyto C activates the caspase-dependent apoptotic pathway. Hence, ROS generation and MTP reduction dominate in the activation of the mitochondrial apoptotic pathway, being consistent with the outcomes of Kasumi-1 cells infected with HO-1 siRNA in our study. Therefore, ROS generation is one of the mechanisms involved in cell apoptosis mediated by HO-1 siRNA. Moreover, HO-1 siRNA contributes to cell apoptosis by reducing MTP to activate the mitochondrial apoptotic pathway.

We have demonstrated that both endoplasmic reticulum and mitochondrial apoptotic pathways were associated with Ca^{2+} accumulation and ROS generation, which were involved in cell apoptosis mediated by HO-1 siRNA. However, whether there was a relationship between them remained unclear. Therefore, antioxidant NAC or (and) Ca^{2+}-chelating agent BAPTA-AM were employed to pretreat Kasumi-1 cells to block ROS generation or (and) Ca^{2+} accumulation mediated by HO-1 siRNA, and then the expressions of apoptosis-related proteins and apoptotic rate were detected. NAC and BAPTA-AM treatments could decrease ROS generation and Ca^{2+} accumulation. In addition, cell apoptotic rate, expression of caspase-12 and cytoplasm-Cyto C were reduced, which became more obvious after combined treatment. Therefore, NAC and BAPTA-AM could protect Kasumi-1 cells from apoptosis mediated by HO-1 siRNA, and HO-1 siRNA might affect the viability of Kasumi-1 cells through the interaction between Ca^{2+} and ROS. However, other possibilities cannot be completely excluded. Since cell apoptosis remained when Ca^{2+}-ROS-dependent pathways were blocked, other pathways might exist. For instance, the Fas-FasL pathway might be involved because the expression of caspase-8, the effector caspase activating this pathway, was increased in Kasumi-1 cells infected with HO-1 siRNA.

In conclusion, the potential mechanism for the apoptosis of Kasumi-1 cells mediated by HO-1 siRNA was postulated (Fig. 10). In this study, the mechanisms for cell apoptosis promoted by HO-1 siRNA were preliminary discussed. On one hand, HO-1 siRNA activated the endoplasmic reticulum apoptotic pathway by destroying endoplasmic reticulum homeostasis, releasing Ca^{2+} and activating caspase-12. On the other hand, HO-1 siRNA increased ROS generation and reduced MTP by undermining the steady state of oxidation-reduction system, thus releasing Cyto C and increasing caspase-9 to activate the mitochondrial apoptotic pathway through caspases activation. These two apoptotic pathways enhanced the cleavage function of caspase-3 and PARP, and participated in the biological events promoted by HO-1 siRNA, during which Ca^{2+} and ROS interacted and were interdependent, thus affecting the activation of apoptotic pathways. The findings herein provide theoretical basis for clarifying whether HO-1 is the target of AML treatment and provide a novel protocol for the treatment of AML. Nevertheless, the specific mechanism for the AML cell apoptosis mediated by HO-1 siRNA still needs to be unraveled.

Acknowledgements

References

1. Wang YY, Zhou GB, Yin T, et al: AML1-ETO and C-KIT mutation/overexpression in t(8;21) leukemia: implication in stepwise leukemogenesis and response to Gleevec. Proc Natl Acad Sci USA 102: 1104-1109, 2005.
2. van Besien K: Allogeneic transplantation for AML and MDS: GVL versus GVHD and disease recurrence. Hematology Am Soc Hematol Educ Program 2013: 56-62, 2013.
3. Alam J and Cook JL: How many transcription factors does it take to turn on the heme oxygenase-1 gene? Am J Respir Cell Mol Biol 36: 166-174, 2007.
4. Abraham NG and Kappas A: Pharmacological and clinical aspects of heme oxygenase. Pharmacol Rev 60: 79-127, 2008.
5. Furfaro AL, Piras S, Passalacqua M, et al: HO-1 upregulation: a key point in high-risk neuroblastoma resistance to bortezomib. Biochim Biophys Acta 1842: 613-622, 2013.
6. Lee SE, Yang H, Jeong SI, et al: Induction of heme oxygenase-1 inhibits cell death in crotonaldehyde-stimulated HepG2 cells via the PKC-δ-p38-Nrf2 pathway. PLoS One 7: e41676, 2012.
7. Zhang L, Liu YL, Chen GX, et al: Heme oxygenase-1 promotes Caco-2 cell proliferation and migration by targeting CTNND1. Chin Med J 126: 3057-3063, 2013.
8. Kongpetch S, Kukongviriyapan V, Prawan A, et al: Crucial role of heme oxygenase-1 on the sensitivity of cholangiocarcinoma cells to chemotherapeutic agents. PLoS One 7: e34994, 2012.
9. Tibullo D, Barbagallo I, Giallongo C, et al: Nuclear translocation of heme oxygenase-1 confers resistance to imatinib in chronic myeloid leukemia cells. Curr Pharm Des 19: 2765-2770, 2013.
10. Heasman SA, Zaitseva L, Bowles KM, Rushworth SA and Macewan DJ: Protection of acute myeloid leukaemia cells from apoptosis induced by front-line chemotherapeutics is mediated by haem oxygenase-1. Oncotarget 2: 658-668, 2011.
11. Mayerhofer M, Gleixner KV, Mayerhofer J, et al: Targeting of heat shock protein 32(Hsp32)/heme oxygenase-1(HO-1) in leukemic cells in chronic myeloid leukemia: a novel approach to overcome resistance against imatinib. Blood 111: 2200-2210, 2008.
12. Wang JS, Yang C, Fang Q, et al: K562 cell line resistance to nilotinib induced in vitro and preliminary investigation of its mechanisms. Zhonghua Xue Ye Xue Za Zhi 33: 906-910, 2012.
13. Chen C, Wang JS, Qin D, et al: The effect of retrovirus-mediated HO-1 gene on chronic myeloid leukemia resistance cell K562/A02 apoptosis induced by nilotinib. Zhonghua Xue Ye Xue Za Zhi 33: 383-387, 2012.
14. Wang JS, Chai BS, Fang Q, et al: Effects of HO-1 gene expression on proliferation of imatinib resistant CML cells. Zhonghua Xue Ye Xue Za Zhi 32: 388-391, 2011.

15. Ma D, Fang Q, Li Y, *et al*: Crucial role of heme oxygenase-1 in the sensitivity of acute myeloid leukemia cell line Kasumi-1 to ursolic acid. Anticancer Drugs 25: 406-414, 2014.
16. Momoi T: Caspases involved in ER stress-mediated cell death. J Chem Neuroanat 28: 101-105, 2004.
17. Ferri KF and Kroemer G: Organelle-specific initiation of cell death pathways. Nat Cell Biol 3: E255-E263, 2001.
18. Xu W, Charles IG and Moncada S: Nitric oxide: orchestrating hypoxia regulation through mitochondrial respiration and the endoplasmic reticulum stress response. Cell Res 15: 63-65, 2005.
19. Choi JA, Lim YJ, Cho SN, *et al*: Mycobacterial HBHA induces endoplasmic reticulum stress-mediated apoptosis through the generation of reactive oxygen species and cytosolic Ca²⁺ in murine macrophage RAW 264.7 cells. Cell Death Dis 4: e957, 2013.
20. Gogvadze V, Norberg E, Orrenius S and Zhivotovsky B: Involvement of Ca²⁺ and ROS in alpha-tocopheryl succinate-induced mitochondrial permeabilization. Int J Cancer 127: 1823-1832, 2010.
21. Akopova OV, Kolchynskaya LY, Nosar' VY, *et al*: The effect of permeability transition pore opening on reactive oxygen species production in rat brain mitochondria. Ukr Biokhim Zh 83: 46-55, 2011.
22. Chatterjee S, Kundu S, Sengupta S and Bhattacharyya A: Divergence to apoptosis from ROS induced cell cycle arrest: effect of cadmium. Mutat Res 663: 22-31, 2009.
23. Li Z and Xing D: Mitochondrial pathway leading to programmed cell death induced by aluminum phytotoxicity in *Arabidopsis*. Plant Signal Behav 5: 1660-1662, 2010.
24. Göke R, Göke A, Göke B and Chen Y: Regulation of TRAIL-induced apoptosis by transcription factors. Cell Immunol 201: 77-82, 2000.
25. Lundvig DM, Immenschuh S and Wagener FA: Heme oxygenase, inflammation, and fibrosis: the good, the bad, and the ugly? Front Pharmacol 3: 81, 2012.
26. Verkhratsky A and Toescu EC: Endoplasmic reticulum Ca²⁺ homoestasis and neuronal death. J Cell Mol Med 7: 351-361, 2003.
27. Nakagawa T, Zhu H and Morishima N: Caspase-12 mediates endoplasmic-reticulum-specific apoptosis and cytotoxicity by amyloid-beta. Nature 403: 98-103, 2000.
28. Maines MD, Ibrahim NG and Kappas A: Solubilization and partial purification of heme oxygenase from rat liver. J Biol Chem 252: 5900-5903, 1997.
29. Kim JS, Wang JH and Lemasters JJ: Mitochondrial permeability transition in rat hepatocytes after anoxia/reoxygenation: role of Ca²⁺-dependent mitochondrial formation of reactive oxygen species. Am J Physiol Gastrointest Liver Physiol 302: G723-G731, 2012.
30. Lee HZ, Liu WZ, Hsieh WT, *et al*: Oxidative stress involvement in Physalis angulata-induced apoptosis in human oral cancer cells. Food Chem Toxicol 47: 561-570, 2009.
31. McGill A, Frank A, Emmett N, *et al*: The anti-psoriatic drug anthralin accumulates in keratinocyte mitochondria, dissipates mitochondrial membrane potential, and induces apoptosis through a pathway dependent on respiratory competent mitochondria. FASEB J 19: 1012-1014, 2005.